Development 140, 1342-1352 (2013) doi:10.1242/dev.080630

Dynamic temporal requirement of *Wnt1* in midbrain dopamine neuron development

Jasmine Yang[1,*], Ashly Brown[2,*], Debra Ellisor[1,*], Erin Paul[3], Nellwyn Hagan[2] and Mark Zervas[1,‡]

SUMMARY

Wnt1-expressing progenitors generate midbrain dopamine (MbDA) and cerebellum (Cb) neurons in distinct temporal windows and from spatially discrete progenitor domains. It has been shown that *Wnt1* and *Lmx1a* participate in a cross-regulatory loop that is utilized during MbDA neuron development. However, *Wnt1* expression dynamically changes over time and precedes that of *Lmx1a*. The spatial and temporal requirements of *Wnt1* in development and specifically its requirement for MbDA neurons remain to be determined. To address these issues, we generated a conditional *Wnt1* allele and temporally deleted *Wnt1* coupled with genetic lineage analysis. Using this approach, we show that patterning of the midbrain (Mb) and Cb by *Wnt1* occurs between the one-somite and the six- to eight-somite stages and is solely dependent on *Wnt1* function in the Mb, but not in the Cb. Interestingly, an *En1*-derived domain persists after the early deletion of *Wnt1* and mutant cells express OTX2. However, the *En1*-derived *Wnt1*-mutant domain does not contain LMX1a-expressing progenitors, and MbDA neurons are depleted. Thus, we demonstrate an early requirement of *Wnt1* for all MbDA neurons. Subsequently, we deleted *Wnt1* in the ventral Mb and show a continued late requirement for *Wnt1* in MbDA neuron development, but not in LMX1a-expressing progenitors. Specifically, *Wnt1* deletion disrupts the birthdating of MbDA neurons and causes a depletion of MbDA neurons positioned medially and a concomitant expansion of MbDA neurons positioned laterally during embryogenesis. Collectively, our analyses resolve the spatial and temporal function of *Wnt1* in Mb and Cb patterning and in MbDA neuron development *in vivo*.

KEY WORDS: Wnt1, Conditional knockout, Dopamine neurons, Genetic inducible fate mapping, Midbrain, Neural development, Mouse

INTRODUCTION

The midbrain (Mb) comprises the superior colliculus, which integrates attention and visual stimuli, and the inferior colliculus, which is an obligate auditory processing center. These dorsal Mb (d.Mb) structures are adjacent to the cerebellum (Cb), which controls motor behaviors. The ventral Mb (v.Mb) contains molecularly, physiologically and biochemically distinct neurons that control complex functions. Of particular interest are the Mb dopamine (MbDA) neurons because they modulate brain function and are centrally involved in schizophrenia, addiction and Parkinson's disease. During embryogenesis, MbDA neurons are derived from multiple lineages originating within the mesencephalon (mes), which is the Mb primordium (Zervas et al., 2004; Joksimovic et al., 2009; Brown et al., 2011; Hayes et al., 2011; Blaess et al., 2011). The molecular identity of the mes is based on a combinatorial code of transcription factors and is patterned by signaling molecules, including WNT1 (reviewed by Zervas et al., 2005). We investigated *Wnt1*, which is initially expressed broadly in the mes, but becomes restricted to distinct domains over time (Wilkinson et al., 1987; Echelard et al., 1994; Zervas et al., 2004). Mice with a null allele of *Wnt1* or with a spontaneous mutation in *Wnt1* do not form the Mb and Cb, demonstrating the importance of WNT1 for these domains (McMahon and Bradley, 1990; McMahon et al., 1992; Thomas et al., 1991; Bally-Cuif et al., 1995; Ellisor et al., 2012). WNT1 functions through β-catenin-mediated WNT signaling and β-catenin regulates cell cycle exit and MbDA neuron development (Tang et al., 2009; Tang et al., 2010). In addition, β-catenin binds to the promoter of *Lmx1a*, which is proposed to be a determinant of MbDA neurons (Andersson et al., 2006; Chung et al., 2009). However, all WNTs that use canonical signaling converge on β-catenin, which precludes an understanding of the specificity of WNT ligand involvement in MbDA neuron development *in vivo*. Genetic inducible fate mapping (GIFM) shows that distinct spatial and temporal epochs underpin *Wnt1* lineage contribution to MbDA neurons and to Cb neurons (Brown et al., 2011; Hagan and Zervas, 2012). Furthermore, dynamic oscillatory genetic networks in human neuronal progenitors are influenced by WNT1 (Wexler et al., 2011). However, the functional requirement of WNT1 in developmental processes is unresolved. Thus, we generated a conditional knockout allele of *Wnt1* that we coupled with GIFM to uncover distinct spatial and temporal requirements for *Wnt1* in patterning the Mb and Cb, controlling ventral mesencephalon (v.Mes) progenitors and regulating cell cycle exit during MbDA neuron development.

MATERIALS AND METHODS

Wnt1 conditional knockout targeting construct (*pWnt1^{neoflox}*)

Wnt1 conditional knockout constructs were generated by recombineering (supplementary material Fig. S1) (Liu et al., 2003). Briefly, we captured *Wnt1* and modified it by placing a *loxP-PGK-gb2-neo-loxP* cassette between the third and fourth exons (*LoxP*) (supplementary material Fig. S1A,B, Table S1). Recombinants were determined by positive selection followed by pKS-Cre removal of the *Neo* cassette. A second *FRT-PGK-gb2-neo-FRT-loxP* cassette was inserted between the first and second exons (*LoxP-FRT*; Table 1) and was used for selection in embryonic stem (ES) cells. The targeting vector was designated as *pWnt1^{neoflox}* (supplementary material Fig. S1B). Plasmids were verified by PCR, restriction digestion and sequencing. The recombination potential of *pWnt1^{neoflox}* was determined by expressing it in *Escherichia coli* cells electroporated with *pKS-Cre*, resulting in the deletion of exons 2 and 3 (supplementary material Fig. S1C).

[1]Department of Molecular Biology, Cell Biology and Biochemistry, [2]Department of Neuroscience, [3]Brown University Transgenic Facility, Division of Biology and Medicine, Brown University, 70 Ship Street, Providence, RI 02903, USA.

*These authors contributed equally to this work
‡Author for correspondence (Mark_Zervas@brown.edu)

Accepted 10 January 2013

Gene targeting and conditional gene manipulations

JM8.F6 ES cells of C57Bl/6 origin (generously provided by Dr Bill Skarnes) (Pettitt et al., 2009) were electroporated with 20 μg of linearized *pWnt1*^{neoflox}. G418-resistant clones were confirmed by PCR screening for the *Neo* cassette (primers 3, 5) and positive clones were screened for the absence of the *AMP* cassette by PCR (primers 9, 10). Clones were also screened for the downstream *loxP* site (primers 1, 2). Primer sequences are provided in supplementary material Table S2. Two correctly targeted ES clones, PL1G10 and PL1G12, were karyotyped as 95% normal and used for blastocyst injection. Correctly targeted *Wnt1*$^{neoflox/+}$ founders were derived from germ line chimeras and bred to *Flpe* mice (The Jackson Laboratory #003946) to delete the *Neo* cassette. Subsequent matings eliminated the *Flpe* allele to generate the *Wnt1*^{flox} allele (*Wnt1*^{fl}). *Wnt1*$^{fl/+}$ or *Wnt1*$^{fl/fl}$ mice were bred with the following lines: (1) *En1*^{Cre} for early [starting at embryonic day (E) 8.0] cumulative recombination (Kimmel et al., 2000; Chi et al., 2003; Ellisor et al., 2009); (2) *Gbx2*$^{CreER\text{-}ires\text{-}eGFP}$ (Chen et al., 2009; Luu et al., 2011) and (3) *Wnt1-CreER* plus tamoxifen for temporal control of recombination (Zervas et al., 2004; Brown et al., 2011); (4) *Shh*^{Cre} for cumulative recombination starting at E9.0-9.5 (Harfe et al., 2004; Hayes et al., 2011). Tamoxifen takes 6 hours to initiate recombination and lasts for 24-30 hours (reviewed by Ellisor et al., 2009; Brown et al., 2009). Genotyping was carried out as previously described (Ellisor et al., 2009). *Rosa26*$^{lox\text{-}STOP\text{-}lox\text{-}tdTomato}$ (*R26*^{tdTomato}) mice were used for lineage tracing and *Wnt1-Venus* mice were used to detect *Wnt1* expression (Madisen et al., 2010; Brown et al., 2011; Ellisor et al., 2012). All *Cre* and reporter lines in this study have been validated and described elsewhere (Kimmel et al., 2000; Li et al., 2002; Zervas et al., 2004; Madisen et al., 2010; Brown et al., 2011; Hagan and Zervas, 2012; Hayes et al., 2011). Mice were housed and handled in accordance with Brown University Institutional Animal Care and Use Committee guidelines.

In situ hybridization, β-galactosidase (β-gal) histochemistry and immunofluorescence immunocytochemistry

Full details of these experimental protocols have been previously published (Ellisor et al., 2009; Brown et al., 2011; Hagan and Zervas, 2012). Primary antibodies for marker analysis were: anti-tyrosine hydroxylase (TH; Chemicon, 1:500), anti-5-hydroxytryptamine (5-HT; Jackson ImmunoResearch, 1:500), anti-OTX2 (Abcam, 1:250), anti-NURR1 (Santa Cruz, 1:200), anti-LMX1a (Michael German, UCSF, 1:1000), anti-GFP (Nacalai Tesque, 1:500) and anti-dsred (1:500, Clontech). Secondary antibodies (Molecular Probes, 1:500) were: donkey anti-rabbit Alexa 555, donkey anti-rat Alexa 488, donkey anti-rabbit IgG-Alexa488, donkey anti-goat IgG-Alexa488, donkey anti-rabbit IgG-Alexa 350.

Cell cycle analysis

Pregnant dams were given 20 mg/kg 5-ethynyl-2′-deoxyuridine (EdU) by intraperitoneal injection (Wang et al., 2011) and sections were labeled for Ki67 (1:100; rat monoclonal IgG2a; Dako, cat #M7249), TH (1:500; rabbit polyclonal IgG; Millipore-Chemicon, cat #AB152), RFP (1:1000; chicken polyclonal IgG; VWR, cat #RL600-901-379), EdU (Click-iT EdU Alexa Fluor 647 Imaging Kit; Invitrogen, cat #C10340) and Hoechst. EdU staining was carried out following the manufacturer's instructions. Antigen retrieval was carried out for Ki67 immunolabeling by boiling sections in R-Buffer A (Electron Microscopy Sciences) and neutralizing with 0.1 M borate buffer. Secondary antibodies (1:500) were: Alexa 488 (donkey anti-rat; Invitrogen, cat #A-21208), Alexa 594 (donkey anti-rabbit; Invitrogen, cat #A-11012), Alexa 555 (goat anti-chicken; Invitrogen, cat #A-21437). Sections were imaged using a Zeiss LSM 710 Confocal Laser Scanning Microscope (lasers for excitation at 405 nm, 488 nm, 561 nm, 594 nm and 633 nm) with a 40× water immersion objective (NA 1.20) and a 1.3× zoom. *z*-series stacks were captured at 1-μm intervals and processed with ZEN 2009 software. Images were acquired with a 34-channel QUASAR detector set to collect emitted light of specific wavelengths. Beam splitters were optimized to collect fluorescent signals: dsred (Alexa 555, imaged using the 561 laser, a collection window of 569-598 nm, and one beam splitter for 488 nm/561 nm); Hoechst and TH [Alexa 594, imaged simultaneously with 594 nm and 405 nm lasers, collection windows at 426-589 nm (Hoechst) and 598-646 nm (Alexa 594), and two beam splitters for 488 nm/594 nm and 405 nm]. Ki67 and EdU [Alexa 488 and Alexa 647 were imaged simultaneously with 488 nm and 633 nm lasers, respectively, collection windows at 501-550 nm (Alexa 488) and 646-695 nm (Alexa 647), and one beam splitter for 488 nm/561 nm/635 nm signal]. Fluorescent signals did not bleed through into other channels. Pinhole settings for image acquisition were 30 μm (405 nm and 594 nm lasers), 34 μm (561 nm laser) and 31 μm (488 nm and 633 nm lasers). The ventricular zone (outer layer of v.Mes) and the differentiated zone (inner layer of v.Mes) at rostral, intermediate and caudal locations were sampled by collecting six *z*-series stacks: (1) rostral-inner, (2) rostral-outer, (3) intermediate-inner, (4) intermediate-outer, (5) caudal-inner, (6) caudal-outer using a 166 × 166 μm optical dissector (Fig. 6; supplementary material Fig. S9). Three medial, three off-midline and three lateral sagittal sections were identified as described previously (Brown et al., 2011) and sampled to obtain medial-to-lateral slabs. Marker positive cells were counted from *Shh*^{Cre};*Wnt1*$^{\Delta vMes/+}$;*R26*^{tdTomato} (n=5), *Shh*^{Cre};*Wnt1*$^{\Delta vMes/\Delta vMes}$;*R26*^{tdTomato} or *Shh*^{Cre};*Wnt1*$^{\Delta vMes/\Delta vMes}$ embryos (n=4). Cell counts from animals of matched genotypes were summed (total count) and the total counts for each animal were averaged. A two-tailed t-test was used to analyze cell counts and to determine statistical significance (P-values are indicated in text).

Microdissection and fluorescence-activated cell sorting (FACS)

The v.Mes of *Wnt1-Venus* embryos was microdissected as previously described (Brown et al., 2009; Ellisor et al., 2012). Briefly, we isolated the v.Mes under a stereofluorescence microscope. The small domain of YFP-expressing cells was carefully dissected away from the posterior mes 'ring' and dorsal tissue. In addition, d.Mes or whole head was isolated. The isolated issues were trypsinized using TryplE Express (Gibco) and DNase (Roche) at 1:1000 for 8 minutes at 37°C. Subsequently, 10% FBS in PBS was added to stop the reaction. Samples were then mechanically dissociated using a 20-gauge needle and 1cc syringe to generate a single cell suspension. Cells were stored on ice until sorting with a FACSAria flow cytometer (BD Biosciences) and analyzed using Diva software (BD Biosciences) at Brown University's Flow Cytometry and Sorting Facility. Population gates were established by setting threshold values based on wild-type littermate control samples and negative control samples obtained from the prosencephalon. Cells were sorted into clean epitubes containing a small volume of 10% FBS in PBS and spun at 3000 rpm (800 ***g***) for 10 minutes at 4°C. PBS was removed and 100 μl of Trizol (Invitrogen) was added and samples were stored at –80°C until RNA extraction.

Quantitative reverse transcriptase polymerase chain reaction (qRT-PCR)

Cells in Trizol were thawed on ice and allowed to sit at room temperature for 5 minutes. Chloroform (25 μl) was added to each tube and shaken vigorously for 15 seconds and incubated at room temperaturefor 2-3 minutes. Samples were centrifuged at 4°C for 15 minutes. RNA was transferred to a new tube and isopropanol (50 μl) was added and incubated for 10 minutes at room temperature. Samples were spun at 13,200 rpm (16,100 ***g***) for 15 minutes at 4°C. The RNA pellet was washed with 250 μl of 75% ethanol, spun at 7500 rpm (5100 ***g***) for 5 minutes at 4°C, and resuspended in 20 μl of dH_20. RNA was quantified with a nanodrop and assed for purity with an Agilent Bioanalyzer. cDNA was synthesized using iScript cDNA Synthesis Kit (BioRad #170-8890) according to manufacturer's instructions. We used 0.5 μg of RNA template, 4 μl of 5× iScript reaction mix, 1 μl of iScript reverse transcriptase (RT) in a 15 μl reaction. The thermocycle program was 25°C for 5 minutes, 42°C for 30 minutes, 85°C for 5 minutes. qRT-PCR was performed with SYBR Green (Applied Biosystems #4367659) in MicroAmp 96-well reaction plates. For each primer set, we used a reaction mix of nuclease-free water (7.5 μl), Primer 1 (2.0 μl), Primer 2 (2.0 μl), SYBR Green (12.5 μl). Note that all primers were tested to ensure that they yielded a single amplicon of appropriate size (typically ~200 nucleotides). All samples were processed in triplicate and dissociation curves were compared with those obtained for 18S. Relative RNA levels (average±s.d.) were plotted using Numbers; statistical significance was determined using Student's t-test (P<0.05). Primer sequences are provided in supplementary material Table S3.

RESULTS

Dynamic expression of *Wnt1* in MbDA neuron progenitors

We examined *Wnt1* at well-defined stages of MbDA neuron development (Ang, 2006) and focused on v.Mes progenitors because they are a substantial source of MbDA neurons *in vivo* (Brown et al., 2011). We used a genetics-based approach that has been instructive in assessing dynamic gene regulation in spinal cord (Luu et al., 2011). Specifically, we administered tamoxifen at E9.5 to pregnant females harboring *Wnt1-CreER;R26*^{tdTomato}*;Wnt1-Venus* embryos followed by analysis 48 hours later (Fig. 1). In this short-term GIFM experiment, the *Wnt1-CreER;R26*^{tdTomato} allelic combination plus tamoxifen marked the *Wnt1*-expressing progenitor pool at E9.5 whereas the *Wnt1-Venus* transgene showed 'current' *Wnt1* expression at the stage of analysis (E11.5). *Wnt1-CreER;R26*^{tdTomato}*;Wnt1-Venus* embryos had *Wnt1* lineage-derived cells (red fluorescence$^+$) that were GFP$^-$ in the dorsal mesencephanlon (d.Mes), indicating that *Wnt1* expression in these progenitors had ceased over the 2 days following marking (Fig. 1A-C). By contrast, the *Wnt1* lineage in the v.Mes appeared to be double positive (red fluorescence$^+$/GFP$^+$), suggesting that *Wnt1* expression in v.Mes progenitors persisted (Fig. 1A-C). We analyzed the v.Mes by double immunolabeling with an anti-dsred antibody to identify the *Wnt1* lineage (dsred$^+$, red) and an anti-GFP antibody to identify *Wnt1*-expressing progenitors (GFP$^+$, green) (Fig. 1D,E). In medial sections, much of the *Wnt1* lineage marked at E9.5 continued to express *Wnt1* (dsred$^+$/GFP$^+$, yellow cells) (Fig. 1D). However, off-midline sections showed heterogeneity of progenitors: *Wnt1*-lineage derived cells closest to the v.Mes flexure were dsred$^+$/GFP$^+$ (Fig. 1E, yellow cells) interspersed amongst cells expressing GFP only (Fig. 1E, white arrowheads). Cells proximal to the ventricle were dsred$^+$ (Fig. 1E, purple arrowheads). Interestingly, MbDA neurons (tyrosine hydroxylase, TH$^+$) at E11.5 were located in the differentiated zone at the v.Mes flexure and were derived from the *Wnt1* lineage and continued to express *Wnt1* (Fig. 1F,G; TH$^+$/dsred$^+$/GFP$^+$, blue arrowheads). In addition, we observed clonal-like cohorts of cells that had expressed *Wnt1* at E9.5 but had ceased to express *Wnt1* by E11.5 (Fig. 1F,G; dsred$^+$/GFP$^-$, purple arrowheads), and clones that appeared to newly express *Wnt1* (Fig. 1F,G; dsred$^-$/GFP$^+$, white arrowheads). One caveat of this last group is that some cells may have escaped marking owing to the mosaic nature of CreER-tamoxifen. We observed a similar dynamic regulation when we administered tamoxifen at E8.5 and analyzed E12.5 embryos, with the exception of the marked *Wnt1* lineage being more broadly distributed throughout the mes (data not shown). Thus, there was a cohort of the *Wnt1* lineage that expressed *Wnt1* early and then extinguished *Wnt1* over the following 2-4 days and cells that expressed *Wnt1* early and continued to express *Wnt1*. These findings showed dynamic regulation of *Wnt1* and suggested distinct temporal roles for *Wnt1* in development.

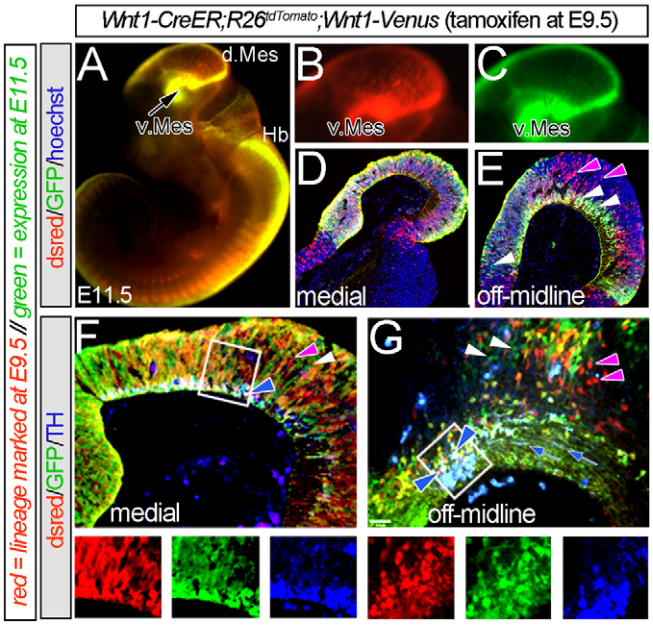

Fig. 1. Dynamic regulation of *Wnt1* expression. (**A-C**) *Wnt1-CreER;R26*^{tdTomato}*;Wnt1-Venus* embryo at E11.5 with *Wnt1* lineage marked at E9.5 (dsred$^+$) and 'current' *Wnt1*-expressing progenitors (YFP$^+$, green). (**D**,**E**) Immunolabeling of the *Wnt1* lineage (dsred$^+$, red) and *Wnt1*-expressing progenitors (GFP$^+$, green) in the v.Mes. Purple arrowheads indicate progenitors that expressed *Wnt1* at E9.5 and ceased to express *Wnt1* (red cells); white arrowheads indicate progenitors that newly turned on *Wnt1* (GFP$^+$); yellow cells are progenitors that expressed *Wnt1* early and continued to express *Wnt1*. (**F**,**G**) MbDA neurons (TH$^+$, blue) derived from the *Wnt1* lineage (red) continued to express *Wnt1* (green) (TH$^+$/dsred$^+$/GFP$^+$, blue arrowheads). Lower panels in F,G show single channels of MbDA neurons from regions of interest (boxes). Purple arrowheads indicate cells that expressed *Wnt1* early and then ceased to express *Wnt1*; white arrowheads indicate progenitors that newly turned on *Wnt1*.

Generation of a conditional knockout allele of *Wnt1*

We generated a conditional knockout allele of *Wnt1* using recombineering technology (Liu et al., 2003) to address the temporal requirement of *Wnt1* in development (supplementary material Fig. S1). The entire *Wnt1* gene was captured from a bacterial artificial chromosome (BAC) library (supplementary material Fig. S1A) and modified by cloning a *loxP* site between the third and fourth exons and cloning a *FRT-PGK-gb2-neo-FRT-loxP* cassette between the first and second exons (Fig. 2A; supplementary material Fig. S1B). Linearized *pWnt1*^{neoflox} was electroporated into mouse ES cells and clones that had undergone homologous recombination were used to generate chimeras (Fig. 2A,B). *Wnt1*$^{neoflox/+}$ founders were bred to *Flpe* mice to remove the *Neo* cassette (Fig. 2A,C). To validate the ability to convert the *Wnt1*^{fl} to the deleted allele *in vivo* (designated *Wnt1*$^{\Delta}$), we bred *Wnt1*$^{fl/+}$ males with *En1*^{Cre} females and analyzed the rostral and caudal halves of embryos at the 6- to 8-somite stage (n=3) by PCR, which confirmed the *Wnt1*$^{\Delta}$ allele in embryos that inherited *En1*^{Cre} (supplementary material Fig. S2).

Conditional *Wnt1* deletion disrupts mesencephalon and rhombomere 1 patterning

We generated and bred *En1*^{Cre}*;Wnt1*$^{fl/+}$ to *Wnt1*$^{fl/+}$ mice to conditionally delete *Wnt1* early in midbrain-hindbrain (MHB) development, consistent with *En1* expression and *En1*^{Cre}-mediated recombination (Li et al., 2002; Chi et al., 2003; Ellisor et al., 2009). Operationally and for clarity of discussing the multiple *Cre* lines used in this study, we designated the deleted allele in the MHB as *Wnt1*$^{\Delta MHB}$. *Wnt1*$^{fl/+}$ and *Wnt1*$^{+/+}$ embryos were morphologically normal at E10.5 (n=4) (Fig. 2D; supplementary material Fig. S3). By contrast, *En1*^{Cre}*;Wnt1*$^{\Delta MHB/\Delta MHB}$ conditional mutant littermates (n=3) had a severe deletion of the putative mes and rhombomere 1 (r1) (Fig. 2I; supplementary material Fig. S3). We assayed sagittal sections from controls and conditional mutants by molecular

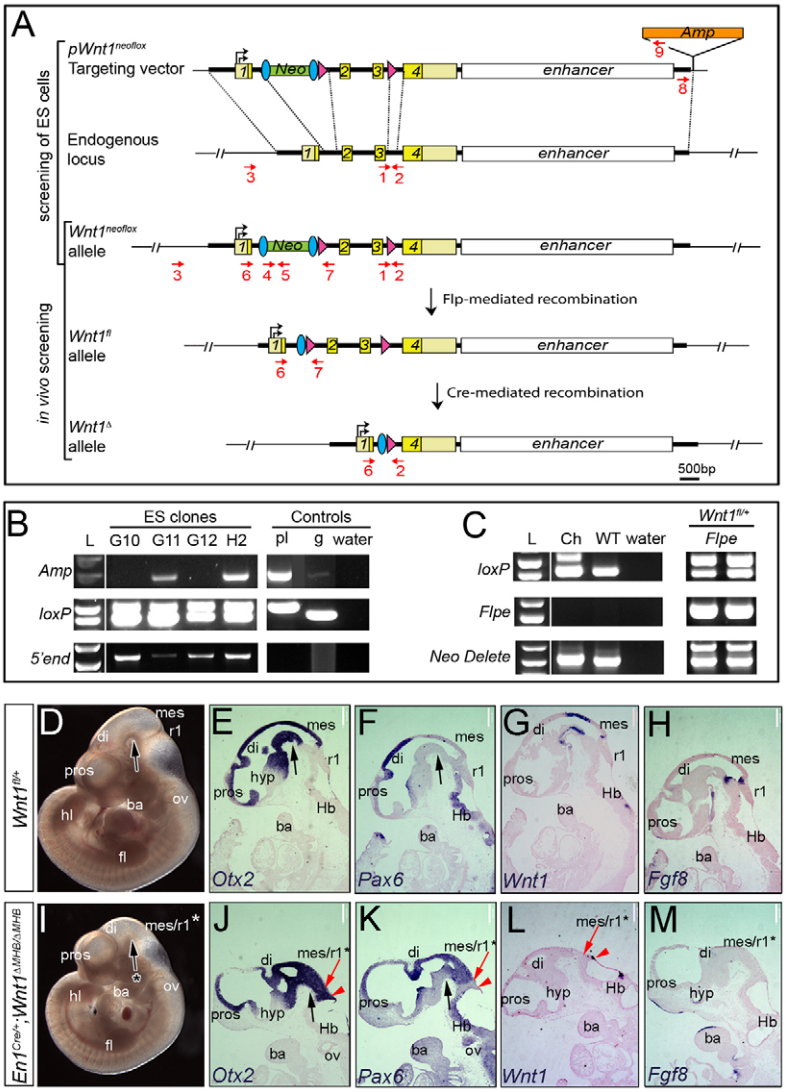

Fig. 2. *Wnt1* conditional knockout allele and conditional deletion of *Wnt1* in the Mb and Hb. (**A**) The targeting vector contained *Frt* (blue ovals) and *loxP* (pink triangles) sites and an *Amp* cassette (orange rectangle). Homologous recombination replaced endogenous *Wnt1* and *Flpe* removed the *Neo* selection cassette (green rectangle). Cre-mediated recombination generates a $Wnt1^{\Delta}$ allele. (**B**) PCR screening of ES cell clones: G10 and G12 did not contain the *Amp* cassette (amplified by primers 9,10), were heterozygous for the downstream *loxP* site (primers 1,2) and were positive for *Neo* (primers 3,5); G11 and H2 did not have the correct profile and were not used. Control plasmid (pl, $pWnt1^{neoflox}$) had an *Amp* cassette and downstream *loxP* site. Genomic DNA (g) produced an amplicon corresponding to *Wnt1* (primers 1,2). (**C**) $Wnt1^{fl/+}$ chimera (Ch) derived from G10 was heterozygous for the downstream *loxP* site (primers 1,2) and had a single amplicon (primers 6,7 *Neo Delete*) that was generated from the wild-type (WT) locus only because *Neo* was large. WT mice produce an amplicon corresponding to the endogenous loci with primer sets 1,2 or 6,7. $Wnt1^{fl/+}$;*Flpe* mice had both *loxP* sites (primers 6,7 and 1,2) and the WT locus. (**D-H**) Control embryos had normal morphology, *Otx2* in the prosencephalon (pros), *Pax6* in the diencephalon (di) and anterior ventral hindbrain (v.Hb). *Wnt1* was in the caudal mes and *Fgf8* was in the isthmus. (**I-M**) $En1^{Cre}$;$Wnt1^{\Delta MHB/\Delta MHB}$ mutants at E10.5 had a depleted mes/r1 (asterisk in I) and truncated v.Mes flexure (arrow in I). (J,K) *Otx2* in the pros, di, remaining mes/r1 (red arrow), and dorsal a.Hb (red arrowhead). *Pax6* overlapped with *Otx2* anteriorly, but not in the mes/r1 (red arrow) or a.Hb (red arrowhead). The $Otx2^{+}$/$Pax6^{-}$ v.Mes (black arrows) was diminished in $En1^{Cre}$;$Wnt1^{\Delta MHB/\Delta MHB}$ embryos. (L,M) *Wnt1* was not detected in remaining mes/r1 (red arrow), but was in lateral r1 (red arrowhead) whereas *Fgf8* was depleted in the a.Hb. ba, branchial arch; fl, forelimb; hl, hind limb; hyp, hypothalamus; ov, otic vesicle.

marker analysis. In controls, *Otx2*, *Pax6*, *Wnt1* and *Fgf8* were expressed in well-defined domains at E10.5, as previously described (Fig. 2E-H; supplementary material Fig. S4A-G). $En1^{Cre}$;$Wnt1^{\Delta MHB/\Delta MHB}$ mutants at E10.5 had *Otx2* expression throughout the prosencephalon and diencephalon but not in the hypothalamus (Fig. 2J), which was similar to controls. *Otx2* was also expressed in the remaining putative mes (Fig. 2J, red arrow) and r1 (Fig. 2J, red arrowhead) based on morphology. *Pax6* delineated the diencephalon, but was not expressed in the remaining putative mes and r1 (Fig. 2K, red arrow and arrowhead, respectively) of conditional mutants. *Wnt1* was not detected in the putative mes, but a small domain was observed in lateral r1 (Fig. 2L, red arrow and arrowhead, respectively) of conditional mutants. The posterior hindbrain (Hb) of $En1^{Cre}$;$Wnt1^{\Delta MHB/\Delta MHB}$ embryos was unaffected because it was outside of the *En1* domain (Fig. 2L). The presence of *Wnt1* in a small lateral r1 domain suggested that $En1^{Cre}$ did not mediate recombination in this territory or that *Wnt1* and *En1* did not overlap in this region. Finally, conditional deletion of *Wnt1* resulted in the absence of *Fgf8* expression in the isthmus (anterior r1) (Fig. 2M). The v.Mes was dysmorphic in mutants and the small portion of the mutant v.Mes flexure was $Otx2^{+}$/$Pax6^{-}$ (Fig. 2J,K versus 2E,F, black arrows; supplementary material Fig. S4).

Early requirement of *Wnt1* in the *En1* lineage

The molecular identity of conditional mutants suggested that some mes/r1 tissue persisted, which prompted us to assess the *En1* lineage in *Wnt1* conditional knockouts by coupling gene deletion and cumulative lineage marking. We compared $En1^{Cre}$;$Wnt1^{\Delta MHB/+}$;$R26^{TdTomato}$ control and $En1^{Cre}$;$Wnt1^{\Delta MHB/\Delta MHB}$;$R26^{TdTomato}$ mutant littermates at E12.5 ($n \geq 3$ each genotype). Whole-mount analysis of controls showed the typical distribution of the *En1* lineage (Fig. 3A-C, red fluorescence). By contrast, $En1^{Cre}$;$Wnt1^{\Delta MHB/\Delta MHB}$;$R26^{TdTomato}$ mutant embryos had a substantial depletion of the *En1* lineage-derived mes (Fig. 3I-K). In addition, r1 was diminished and had only a small domain that was adjacent to axonal bundles connected to the trigeminal ganglia (Fig. 3I). Given that the v.Mes and ventral r1 (v.r1) are where MbDA and serotonin neurons are generated, respectively, we assessed *En1* lineage contribution with biomarkers of neural progenitors and differentiating neurons in these domains (as shown in Fig. 3C,K). The limits of the *En1* lineage delineated the anterior extent of the mes and the posterior limit of r1 in control embryos consistent with previous reports (Fig. 3D-H, arrowheads) (Zervas et al., 2004; Ellisor et al., 2009). OTX2, which plays a role in MbDA neuron development (Di Salvio et al., 2010; Omodei et al., 2008; Vernay et al., 2005) was distributed within the *En1*-derived domain

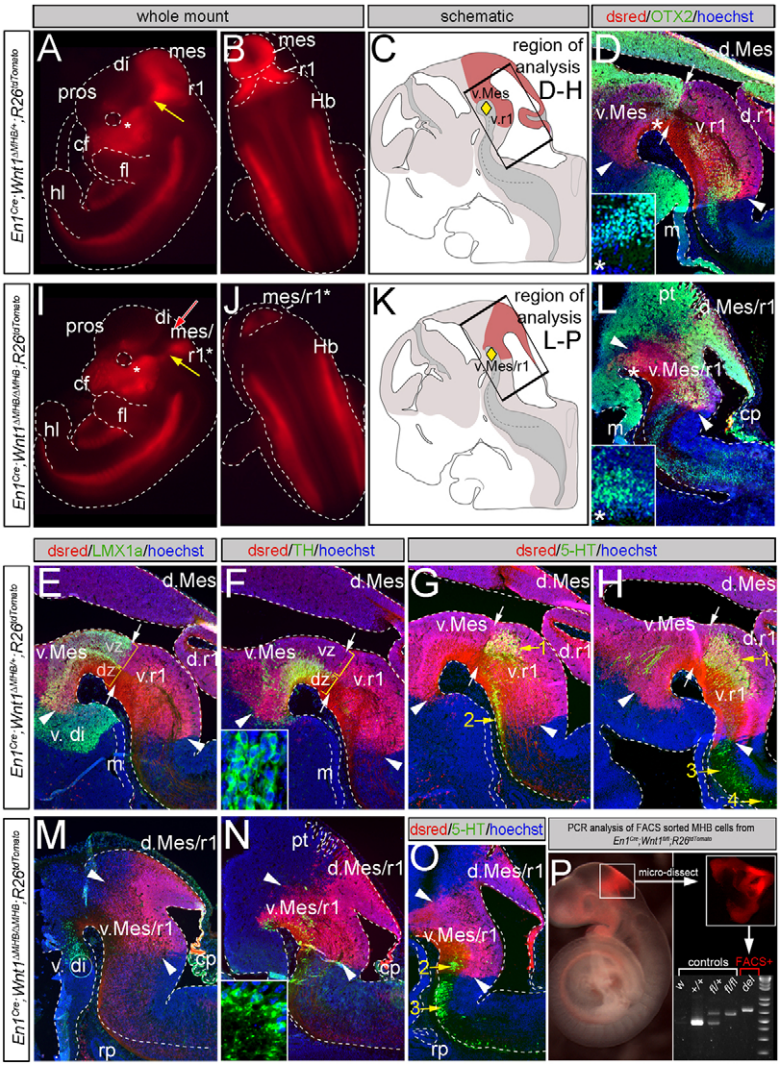

Fig. 3. Early deletion of *Wnt1* depletes MbDA neurons. (**A-H**) $En1^{Cre};Wnt1^{\Delta MHB/+};R26^{tdTomato}$ embryo at E12.5. (A,B) *En1* lineage (red) contribution to the mes, r1, trigeminal ganglia (tg, asterisk) and craniofacial domain (cf). Axons traversed the tg and lateral a.Hb at the pontine flexure (yellow arrow). (C) Region of analysis (black box), v.Mes flexure (diamond) and *En1*-lineage (red shading). (D-H) Control sections immunolabeled for indicated markers (green) and the lineage tracer ($dsred^{+}$, red). *En1*-derived cells were throughout the mes/r1 (delineated by arrowheads). (D) The mes/r1 boundary (arrows) coincided with posterior limit of OTX2. (E) LMX1a in the ventricular zone (vz, yellow bracket) up to the anterior limit of the v.Mes (white arrowheads). (F) MbDA neurons in the differentiated zone (dz, yellow bracket); inset shows TH^{+} neurons at higher magnification. (G,H) 5-HT^{+} neurons in v.r1. Numbers indicate rostral to caudal 5-HT^{+} neurons as indicated in text. (**I-P**) $En1^{Cre};Wnt1^{\Delta MHB/\Delta MHB};R26^{tdTomato}$ mutants at E12.5 (I,J). *Wnt1* mutants were devoid of the mes (indicated by red arrow), but did have a small fused mes/r1 domain (mes/r1*) and sparse projections at the pontine flexure (yellow arrow). (K) Region of analysis and *En1*-lineage (as described for C). (L-P) The *En1*-derived mes/r1 domain (red) was diminished, but a cohort of *En1* lineage-derived cells was present. The anterior boundary was irregular and $dsRed^{+}$ cells were in the di. (L,M) *Wnt1*-mutant/*En1*-lineage derived domain had $OTX2^{+}$ progenitors, but not LMX1a. (N) TH^{+} MbDA neurons were depleted; inset shows sparse TH^{+} neurons. (O) Anterior 5-HT^{+} neurons were depleted whereas those at the edge of the *En1*-lineage domain (2) were diminished and those outside the En1-lineage domain (3) were unaffected. (P) Representative $En1^{Cre};Wnt1^{\Delta MHB/\Delta MHB};R26^{tdTomato}$ embryo with *En1*-lineage derived domain that was microdissected, sorted, and genotyped by PCR: *En1*-derived cells contained only the $Wnt1^{\Delta}$ allele. cp, choroid plexus; di, diencephalon; fl, forelimb; hl, hind limb; m, mammillary body; pros, prosencephalon; pt, pretectum; rp, Rathke's pouch.

and had a sharp caudal limit at the mes/r1 boundary (Fig. 3D, arrows; supplementary material Fig. S5). LMX1a, which is a transcription factor proposed to be a determinant of MbDA neurons (Andersson et al., 2006), was robustly expressed in the ventricular zone and to a lesser extent in the differentiated zone adjacent to the v.Mes flexure with a caudal limit at the v.Mes/v.r1 boundary (Fig. 3E, arrows; supplementary material Fig. S5). LMX1a was also expressed in the ventral diencephalon (Fig. 3E). Tyrosine hydroxylase (TH)-expressing MbDA neurons were located in the differentiated zone of the *En1*-derived v.Mes of controls (Fig. 3F; supplementary material Fig. S5) whereas the cell bodies of 5-hydroxytryptamine (5-HT)-expressing serotonergic neurons were nested within the *En1*-derived r1 and had long anterior-coursing axons that traversed the v.Mes (Fig. 3G,H). *En1* lineage mapping provided insight into the nature of the tissue that remained in $En1^{Cre};Wnt1^{\Delta MHB/\Delta MHB};R26^{TdTomato}$ mutant embryos (Fig. 3L-O, $dsred^{+}$ domain located between arrowheads). The dorsal mes/r1 was severely depleted as evident by the close proximity of the pretectum to putative r1, although the ventral mes/r1 was less affected and had a prominent domain. The *En1*-derived mutant v.Mes contained $OTX2^{+}$ progenitors, but we did not observe $LMX1a^{+}$ progenitors throughout the medial-lateral extent of the v.Mes (Fig. 3L,M; supplementary material Fig. S5). Interestingly, $LMX1a^{+}$ progenitors in the ventral diencephalon that were outside the *En1* domain were also diminished, suggesting a non-cell-autonomous effect resulting from the loss of *Wnt1* within the *En1*-derived domain (Fig. 3M). TH^{+} MbDA neurons in conditional mutants were severely depleted with only a small, disorganized cohort remaining (Fig. 3N; supplementary material Fig. S5). The most rostral 5-HT^{+} neurons (cluster 1) were absent in the remaining *En1*-derived ventral tissue (not shown), although more caudally positioned serotonergic neurons (clusters 2-4) were present (Fig. 3O; data not shown). We microdissected the mes/r1 from $En1^{Cre};Wnt1^{\Delta MHB/\Delta MHB};R26^{TdTomato}$ mutants and used fluorescence-activated cell sorting (FACS) to isolate *En1*-derived ($dsred^{+}$) cells followed by PCR genotyping to detect the status of the *Wnt1* allele. The $dsred^{+}$ cells were $Wnt1^{\Delta/\Delta}$ and did not contain the floxed allele, which indicated that remaining tissue in $En1^{Cre};Wnt1^{\Delta MHB/\Delta MHB};R26^{TdTomato}$ embryos did not require *Wnt1* (Fig. 3P). Collectively, these findings showed that a domain of *En1* lineage-derived v.Mes tissue was established in the absence of *Wnt1*, but that both LMX1a-expressing progenitors and MbDA neurons have an early requirement for *Wnt1*. *En1*-lineage analysis also showed that neurons in the trigeminal ganglia of controls had processes that innervated whisker pads and the craniofacial region and processes that connected to the anterior hindbrain (a.Hb) by

way of the pontine flexure (supplementary material Fig. S6A,B, inset) consistent with previous studies (Ellisor et al., 2009). $En1^{Cre};Wnt1^{\Delta MHB/\Delta MHB};R26^{TdTomato}$ embryos were similar to controls and had trigeminal ganglia projections that innervated the craniofacial region and the pontine flexure (supplementary material Fig. S6C,D). However, analysis of whisker fields (location of vibrissae) and serotonergic innervation of the craniofacial region of conditional knockout embryos showed aberrantly patterned whisker fields innervated by serotonergic neurons and a severe truncation of the *En1*-derived lateral a.Hb (supplementary material Fig. S6C,D,G,H).

Wnt1 in r1 is not required for Cb development and is transiently required for patterning

We previously showed that late temporal epochs of *Wnt1*-expressing progenitors in the rhombic lip of r1 contribute to the Cb, consistent with late *Wnt1* expression in this domain (Hagan and Zervas, 2012). Thus, r1 depletion in $En1^{Cre};Wnt1^{\Delta MHB/\Delta MHB}$ embryos could be due to *Wnt1* function in the mes at the mes/r1 boundary or in the rhombic lip. We addressed this issue by deleting *Wnt1* in the rhombic lip using $Gbx2^{CreER\text{-}ires\text{-}eGFP}$ mice (Chen et al., 2009) plus our $Wnt1^{fl}$ allele and the $R26^{tdTomato}$ line to simultaneously mutate and track the recombination event (Fig. 4A-L). Pregnant dams were treated with tamoxifen at E8.5 to mediate recombination in r1; *Wnt1* was effectively deleted based on molecular analysis to detect the deleted allele and *in situ* hybridization to show loss of *Wnt1* in r1 (Fig. 4A,B,G,H). We evaluated *Gbx2* lineage contribution ($dsred^{+}$) *Gbx2*(GFP), OTX2 and LMX1a expression in r1, which were unaffected by the loss of *Wnt1* (Fig. 4C-F,I-L). Thus, the deletion of r1 was due to *Wnt1* function in the mes and not in the rhombic lip. We next tested the hypothesis that *Wnt1* continues to be required for patterning the mes/r1 and for MbDA neuron development using *Wnt1-CreER* mice (Zervas et al., 2004) coupled with tamoxifen to mediate recombination in *Wnt1*-expressing

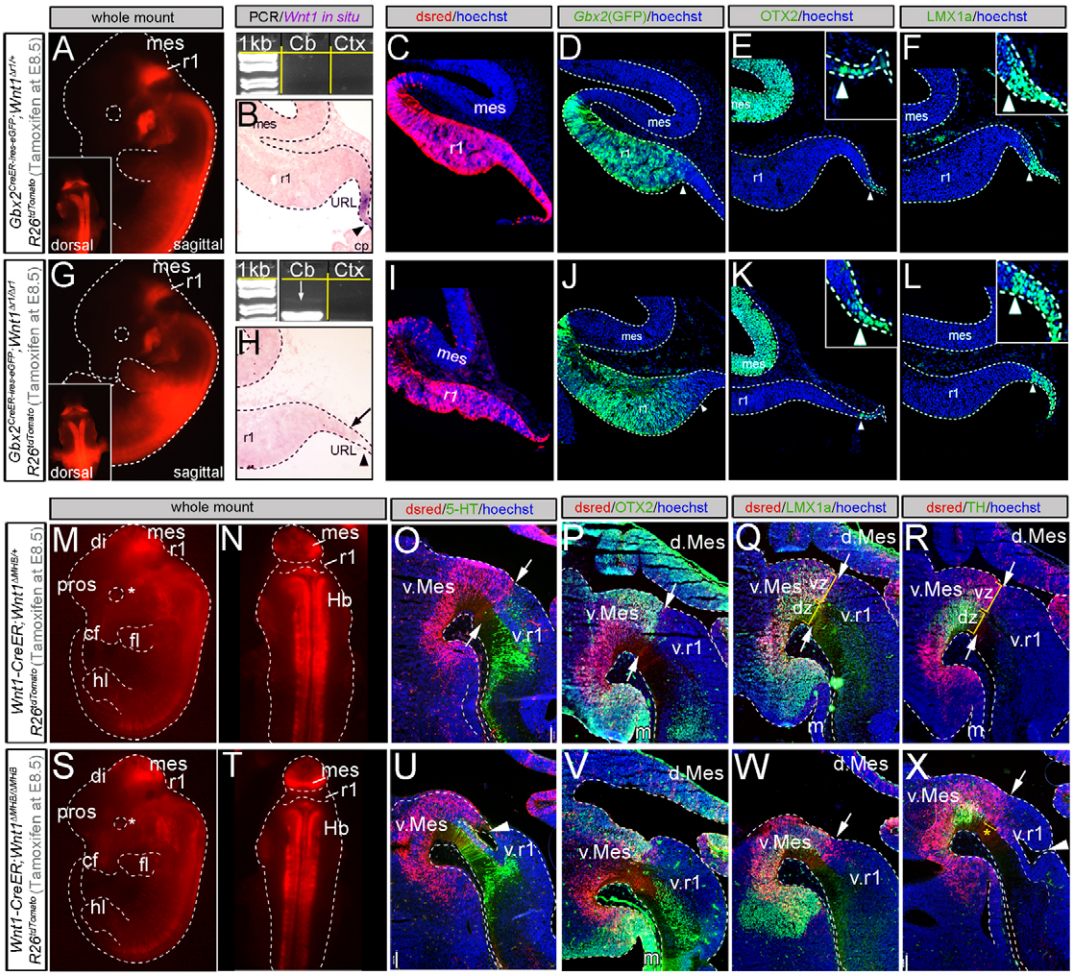

Fig. 4. Temporal requirement of *Wnt1* for patterning the Mb and Cb. (**A-F**) Control E12.5 $Gbx2^{CreER\text{-}ires\text{-}eGFP};Wnt1^{\Delta r1/};R26^{tdTomato}$ embryos received tamoxifen at E8.5 and were analyzed for the *Gbx2* lineage, *Wnt1*, *Gbx2*(GFP), OTX2 and LMX1a. Arrowheads indicate limit of marker expression. (**G-L**) E12.5 $Gbx2^{CreER\text{-}ires\text{-}eGFP};Wnt1^{\Delta r1/\Delta r1};R26^{tdTomato}$ mutants that received tamoxifen at E8.5 had a loss of *Wnt1* in the upper rhombic lip (URL). The *Gbx2* lineage, Gbx2(GFP), OTX2 and LMX1a were unaffected. Arrowheads indicate limit of marker expression. (**M-X**) *Wnt1-CreER*;$Wnt1^{\Delta MHB/+};R26^{tdTomato}$ controls that received tamoxifen at E8.5 and analyzed at E12.5 showed the *Wnt1* lineage (red) in the mes, trigeminal ganglia (asterisk) and craniofacial domain (cf). (O-R) Controls labeled for markers (green) and the lineage tracer ($dsred^{+}$, red) showed *Wnt1*-derived cells throughout the v.Mes, but not in r1. The *Wnt1* lineage abutted 5-HT^{+} neurons in v.r1 and expressed OTX2 and LMX1a in the vz. *Wnt1*-lineage derived TH^{+} neurons in the dz. (S-X) *Wnt1-CreER*;$Wnt1^{\Delta MHB/\Delta MHB};R26^{tdTomato}$ mutants had a smaller v.Mes versus controls although the *Wnt1* lineage (red) was unaffected. 5-HT^{+} neurons were unaffected. *Wnt1*-derived cells expressed OTX2 and LMX1a, but caudal MbDA neurons were depleted (asterisk, bracket in X). cp, choroid plexus; Ctx, cerebral cortex; di, diencephalon; dz, differentiated zone; fl, forelimb; hl, hindlimb; m, mammillary body; pros, prosencephalon; vz, ventricular zone.

progenitors at E8.5 (Fig. 4M-X). *Wnt1*-derived cells (red fluorescence) were similarly distributed in the mes, posterior Hb, and spinal cord in both *Wnt1-CreER;Wnt1*$^{\Delta MHB/+}$*;R26*^{TdTomato} and *Wnt1-CreER;Wnt1*$^{\Delta MHB/\Delta MHB}$*;R26*^{TdTomato} littermates at E12.5 (Fig. 4M,N,S,T). In control embryos, *Wnt1*-derived cells in the v.Mes abutted the 5-HT^{+} neurons in the a.Hb and co-expressed OTX2 and LMX1a (Fig. 4O-Q). TH^{+} MbDA neurons in *Wnt1-CreER;Wnt1*$^{\Delta MHB/+}$*;R26*^{TdTomato} embryos were located in the differentiating zone of the v.Mes with a posterior limit at the mes/r1 boundary (Fig. 4R). The v.Mes in *Wnt1-CreER;Wnt1*$^{\Delta MHB/\Delta MHB}$*;R26*^{TdTomato} embryos was smaller than that in controls and contained an abnormal notch, but was otherwise patterned normally based on the morphology of the v.Mes (Fig. 4U-X). The mutant *Wnt1* lineage marked at E8.5 expressed OTX2 and LMX1a and was distributed similar to controls (Fig. 4V,W). However, the deletion of *Wnt1* at E8.5 resulted in depletion of TH^{+} neurons in the medial v.Mes, but not of 5-HT^{+} neurons in v.r1 (Fig. 4U,X). Interestingly, we also observed an increase in TH^{+} neurons in the off-midline plane of *Wnt1* conditional knockout mutants (data not shown). These phenotypes were observed in two out of four embryos with the variability probably arising from the mosaic nature of recombination with this transgenic line. We also administered tamoxifen to *Wnt1-CreER;Wnt1*$^{\Delta MHB/\Delta MHB}$*;R26*^{TdTomato} embryos at E10.5, which did not result in any overt phenotype in four out of four embryos (supplementary material Fig. S7). These findings indicated that the patterning role of *Wnt1* was early, transient, and restricted to the mes. In addition, a subset of MbDA neurons continued to require *Wnt1* for their development between E8.5 and E10.5.

Wnt1 has a continued role in MbDA neuron development and regulates cell cycle exit

We used the *Shh*^{Cre} line (Harfe et al., 2004; Hayes et al., 2011; Tang et al., 2010; Tang et al., 2009) to address the continued role of *Wnt1* because *Shh*^{Cre} mediates robust and cumulative recombination in the v.Mes beginning at E9.0-9.5 (Harfe et al., 2004; Hayes et al., 2011), which is later than with our *En1*^{Cre} mice. To validate that *Shh*^{Cre} was appropriate to delete *Wnt1* we used FACS to sort v.Mes cells from *Wnt1-Venus* mice (Brown et al., 2011; Ellisor et al., 2012; Hagan and Zervas, 2012) and performed qRT-PCR that showed that *Wnt1*(GFP)-expressing MbDA neuron progenitors also express *Shh* (supplementary material Fig. S8). Because *Shh*^{Cre} mediates recombination in the v.Mes, we operationally define *Wnt1*$^{\Delta vMes}$ as the recombined allele for this experiment (Fig. 5). The *Shh* lineage in E12.5 *Shh*^{Cre}*;Wnt1*$^{\Delta vMes/+}$*;R26*^{TdTomato} embryos analyzed by whole-mount fluorescence and on immunolabeled sagittal sections had a typical distribution of OTX2^{+}, LMX1a^{+} and NURR1^{+} progenitors and early differentiating TH^{+} neurons (Fig. 5A-G). *Shh*^{Cre}*;Wnt1*$^{\Delta vMes/\Delta vMes}$*;R26*^{TdTomato} littermates had a normal distribution of the *Shh* lineage and OTX2^{+}, LMX1a^{+} and NURR1^{+} progenitors (Fig. 5H-L). However, we observed a depletion of medial MbDA neurons and an expansion of more laterally positioned MbDA neurons in mutants (Fig. 5F,G,M,N). Quantification of medial populations revealed TH^{+} counts of 462±103 (mean±s.d.) versus 147±27 from controls and conditional mutants, respectively (n≥4 each genotype), which was a significant decrease in MbDA neurons (Fig. 5O; P=0.0006). By contrast, off-midline TH^{+} counts were 192±51 and 288±45 from control and mutants, respectively, which was a corresponding significant

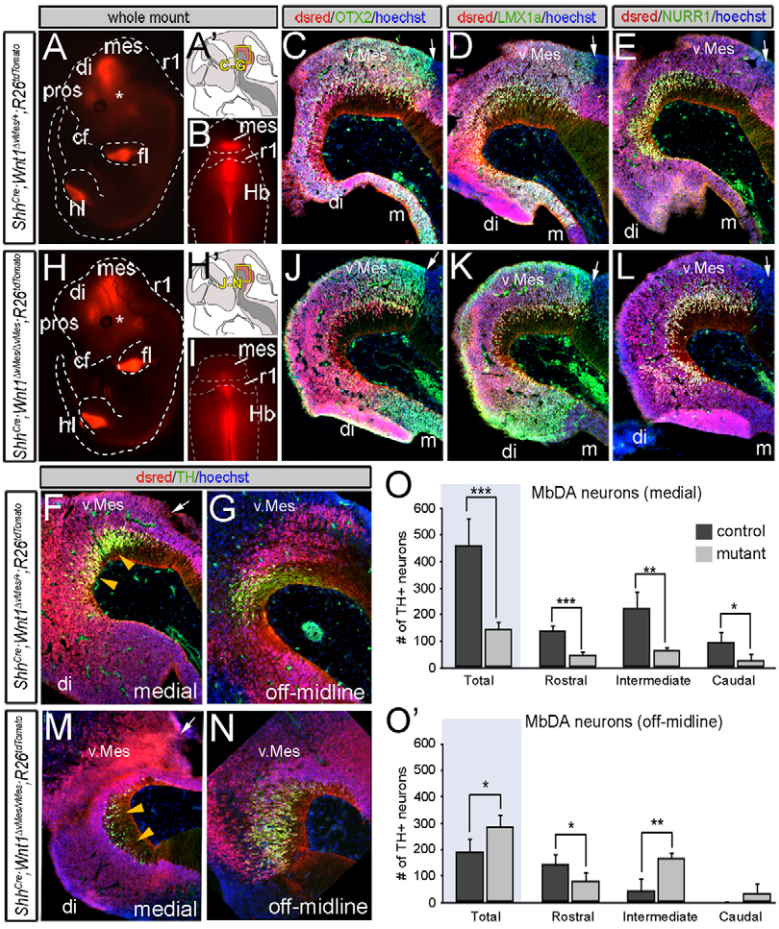

Fig. 5. Late temporal requirement of *Wnt1* for MbDA neuron development. (**A-G**) *Shh*^{Cre}*;Wnt1*$^{\Delta vMes/+}$*;R26*^{tdTomato} controls at E12.5 showed the *Shh* lineage (red) in the v.Mes. (C-G) Sections immunolabeled for indicated markers (green) and the lineage tracer (dsred^{+}, red) showed that the *Shh* lineage expressed OTX2, LMX1a and NURR1. (F,G) *Shh* lineage-derived medial and off-midline TH^{+} neurons. Orange arrowheads indicate TH^{+} neurons. White arrows indicate MHB. Box in A′ indicates the region shown in C-G. (**H-N**) *Shh*^{Cre}*;Wnt1*$^{\Delta vMes/\Delta vMes}$*;R26*^{tdTomato} mutants did not have morphological abnormalities. (J-L) The v.Mes morphology was unaffected and *Shh*-derived cells expressed OTX2, LMX1a and NURR1^{+}, similar to controls. (M,N) Medial TH^{+} MbDA neurons (arrowheads) were severely reduced whereas off-midline TH^{+} neurons were expanded in mutants. White arrows indicate the MHB. (**O**,**O′**) Quantification of TH^{+} MbDA neurons in medial and off-midline planes including rostral to caudal positions from the v.Mes of control and conditional mutants (*P<0.05, **P<0.01, ***P<0.001). Error bars represent s.d. Asterisk in A,H indicates trigeminal ganglia. cf, craniofacial; di, diencephalon; fl, forelimb; hl, hindlimb; m, mammillary body; pros, prosencephalon.

increase of off-midline MbDA neurons (Fig. 5O′; P=0.020). These changes were observed at rostral, intermediate and caudal positions in the v.Mes (Fig. 5O,O′).

MbDA neurons differentiate such that early versus late born neurons occupy more lateral or medial positions, respectively (Kawano et al., 1995; Bayer et al., 1995; Bye et al., 2012). To test whether the MbDA neuron phenotype in $Shh^{Cre};Wnt1^{\Delta vMes/\Delta vMes};R26^{TdTomato}$ embryos was caused by alterations in cell cycle exit we administered EdU at E11.5 and analyzed embryos 24 hours later by confocal microscopy and quantitative analysis to detect Hoechst (nuclear counter stain), dsred (*Shh* lineage), TH (terminally differentiated MbDA neurons), EdU (birthdating) and Ki67 (proliferation) (Fig. 6; supplementary material Fig. S9). $Shh^{Cre};Wnt1^{\Delta vMes/+};R26^{TdTomato}$ controls had 160±33 (mean±s.d.) *Shh* lineage-derived medial MbDA neurons that differentiated at E11.5 ($TH^+/EdU^+/Ki67^-$) (Fig. 6A-F,Y). By contrast, $Shh^{Cre};Wnt1^{\Delta vMes/\Delta vMes};R26^{TdTomato}$ mutants had 38±14 medial MbDA neurons that differentiated at E11.5 ($TH^+/EdU^+/Ki67^-$), which was a significant fourfold reduction (Fig. 6G-L,Y; P=0.0002). Control embryos had negligible 3±3 off-midline $TH^+/EdU^+/Ki67^-$ neurons that differentiated at E11.5 (Fig. 6M-R,Y′) whereas mutant embryos had 38±26, which was a significant increase of MbDA neurons that had differentiated at E11.5 (Fig. 6S-X,Y′; P=0.0200). Both control and mutant embryos had similar counts of proliferating progenitors ($Ki67^+$). However, mutants had significantly more $Ki67^+$ progenitors compared with controls (420±152 versus 155±139, respectively; P=0.0330) in the differentiating zone in medial planes. Finally, we compared the ratio of E11.5 birthdated MbDA neurons ($TH^+/EdU^+/Ki67^-$) to all birthdated cells ($EdU^+/Ki67^-$) to test whether the phenotype we observed was specific to MbDA neurons or the result of global deficits in cell cycle exit. $Shh^{Cre};Wnt1^{\Delta vMes/+};R26^{TdTomato}$ embryos had a $TH^+/EdU^+/Ki67^-$ to $EdU^+/Ki67^-$ ratio of 0.18±0.05 (Fig. 6Z, dark gray bars) whereas $Shh^{Cre};Wnt1^{\Delta vMes/\Delta vMes};R26^{TdTomato}$ embryos had a ratio of 0.05±0.02 (Fig. 6Z, light gray bars), which was a significant reduction (P=0.005). By contrast, the ratio off-midline was 0.01±0.01 for controls (Fig. 6Z′, dark gray bars) and 0.08±0.07 for mutants (Fig. 6Z′, light gray bars), which was a significant increase (P=0.01). The rostral-to-caudal distribution showed similar results (Fig. 6Z,Z′). Thus, the conditional deletion of *Wnt1* resulted in a loss of medial MbDA neurons as well as a smaller fraction of medial cells that differentiated into MbDA neurons and a concomitant larger fraction of ectopic laterally positioned MbDA neurons (Fig. 6AA).

DISCUSSION

Wnt1 is important for Mb and a.Hb development (McMahon and Bradley, 1990; McMahon et al., 1992), but the role of *Wnt1* at specific stages of embryonic development or within specific genetic lineages has been elusive because *Wnt1* mutant mice that were previously available for analysis were derived by neomycin disruption (null alleles) or were caused by a spontaneous mutation (McMahon and Bradley, 1990; McMahon et al., 1992; Thomas and Capecchi, 1990; Thomas et al., 1991). We circumvented these limitations by generating a $Wnt1^{fl}$ allele, which we used in spatial and temporal deletion experiments in combination with genetic lineage tracing. We show that *Wnt1* patterns the d.Mes and v.Mes, and patterns r1 during an early and brief window (~12 hours between 0-1 somites and 6-8 somites). By tracing the *En1* lineage in *Wnt1* conditional mutants, we show that a large portion of *En1*-derived tissue is depleted at E12.5. However, cells derived from the *En1* lineage are present in mutants with a more substantial allotment in v.Mes and v.r1 compared with dorsal tissue. The presence of an *En1*-derived *Wnt1*-mutant domain indicates that a cohort of cells derived from the *En1* lineage does not require *Wnt1*. Thus, the Mb is derived from a heterogeneous pool of progenitors and is partitioned by complex molecular identities and genetic lineages. The deletion of *Wnt1* in the rhombic lip of r1 did not phenocopy the truncation of r1, which provides definitive experimental evidence that *Wnt1* in the mes is functionally required for r1 development, probably by regulating the organizer molecule FGF8.

$OTX2^+$ progenitors persist in *En1*-derived *Wnt1*-mutant v.Mes tissue, suggesting that signaling by *Wnt1* does not induce or maintain *Otx2* at least in a subset of v.Mes cells. This is in contrast to viral-mediated transduction of *Wnt1* in ES cells, which increases *Otx2* mRNA levels (Chung et al., 2009). Thus, *Wnt1* regulation of *Otx2* might be context dependent. The remaining *En1*-derived *Wnt1*-mutant domain is devoid of $LMX1a^+$ cells, suggesting that *Wnt1*-dependent progenitors (which may also be the LMX1a-expressing population) are unable to expand in the absence of *Wnt1* or that a cohort of mutant progenitors may not have been induced resulting in a smaller initial progenitor pool. At the same time, a *Wnt1*-independent population may expand with many of those cells still expressing OTX2. We show that *Wnt1* requirement for $LMX1^+$ progenitors is transient and occurs between the 1-somite and the 6- to 8-somite stages. This finding complements previous observations that *Wnt1*(GFP) is expressed more broadly and prior to LMX1a in the v.Mes (Brown et al., 2011). It has been proposed that *Lmx1a* functions as a determinant of MbDA neurons (Andersson et al., 2006); interestingly, WNT1 uses the canonical β-catenin pathway to regulate *Lmx1a* expression and, conversely, LMX1a binds directly to the promoter of *Wnt1* during MbDA neuron differentiation (Chung et al., 2009). Thus, an alternative explanation for the phenotype of the early deletion of *Wnt1* is that WNT1 initiates *Lmx1a* expression followed by a short pulse of WNT signaling and *Lmx1a*-*Wnt1* cross-regulatory reinforcement. Later, an uncoupling of *Lmx1a* and *Wnt1* might occur in MbDA neuron progenitors, as suggested by results of our conditional deletion of *Wnt1* with *Wnt1-CreER* or Shh^{Cre} lines. This dynamic regulation is consistent with how WNT1 temporally regulates oscillations of gene expression and genetic pathway interactions *in vitro* (Wexler et al., 2011). We also show that even though a v.Mes domain persists with early *Wnt1* deletion, TH^+ neurons are not generated, which is consistent with the absence of LMX1a. Interestingly, medial MbDA neurons have a continued requirement of *Wnt1* for their development that occurs between E8.5 and E10.5. Given that $LMX1a^+$ progenitors are unaffected by the late deletion of *Wnt1*, we suggest that later-born medial MbDA neurons develop independently of LMX1a. The presence of *Wnt1*-dependent/*Lmx1a*-dependent (early) and *Wnt1*-dependent/*Lmx1a*-independent (later) progenitors is consistent with only a subset of MbDA neurons being depleted in *Lmx1a* mutant mice (Ono et al., 2007). Collectively, our findings show that *Wnt1* is a key upstream regulator in MbDA neuron development and that MbDA neurons are derived from progenitors that express *Wnt1* early and continue to express *Wnt1*.

SHH and FGF8 function cooperatively to induce MbDA neurons during a short developmental window and together enhance the efficiency of producing MbDA-like neurons from ES cells and induced pluripotent stem cells (IPSCs) (Ye et al., 1998; Lee et al., 2000; Soldner et al., 2009). *Wnt1*-expressing v.Mes progenitors express components consistent with these signaling pathways and also express *Fzd9* (supplementary material Fig. S8). Thus, we show that MbDA neuron progenitors are poised to respond to SHH, FGF8 and WNT1 signaling. Previous studies have shown that canonical

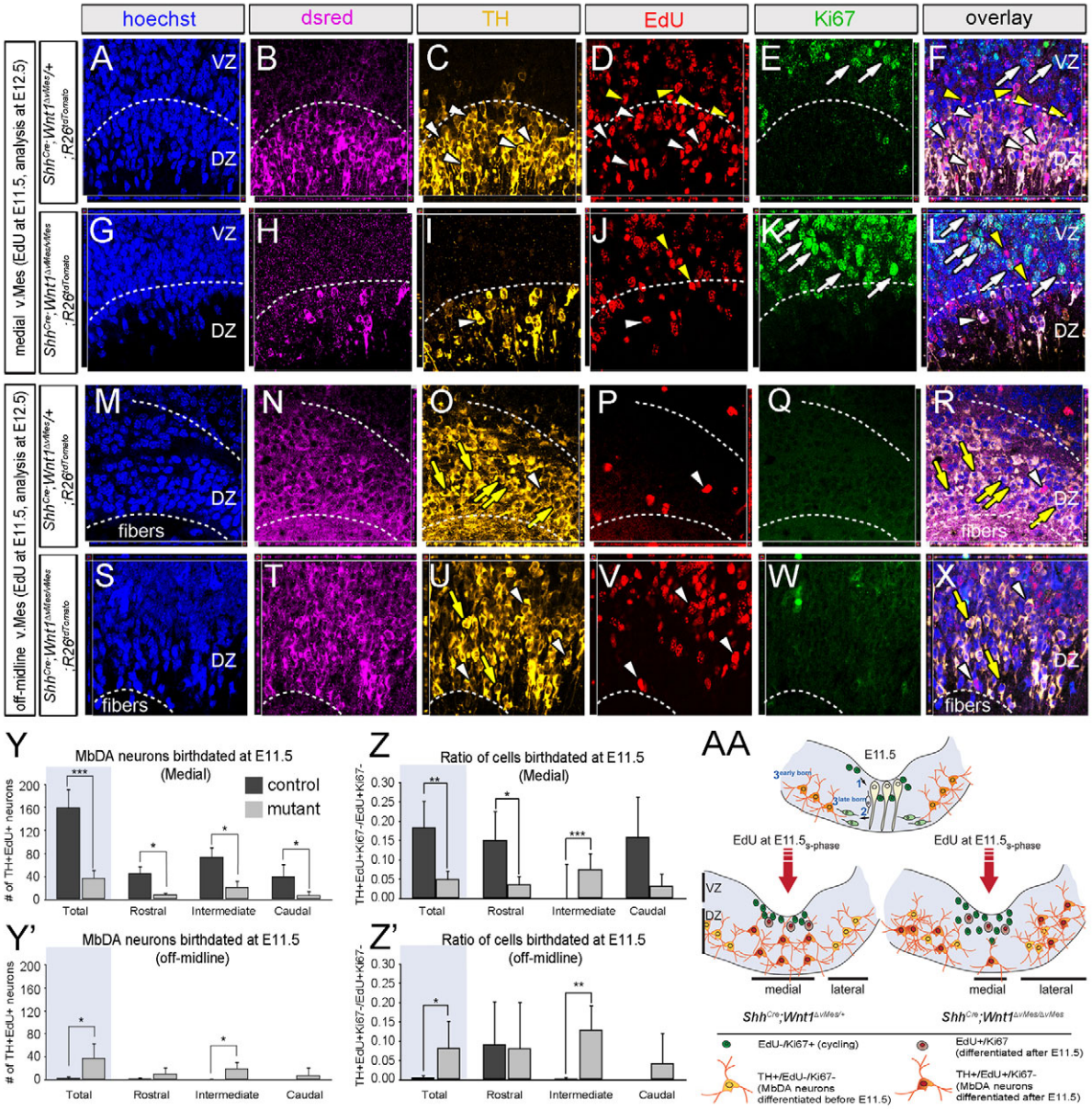

Fig. 6. Late conditional *Wnt1* deletion alters cell cycle exit of MbDA neurons *in vivo*. (**A-X**) EdU was administered at E11.5 and embryos were analyzed at E12.5. (A-F,M-R) $Shh^{Cre};Wnt1^{\Delta vMes/+};R26^{tdTomato}$ controls. (G-L,S-X) $Shh^{Cre};Wnt1^{\Delta vMes/\Delta vMes};R26^{tdTomato}$ mutants. Medial sections (A-L) and off-midline sections (M-X) are shown. Sections were co-labeled for Hoechst (A,G,M,S), dsred (B,H,N,T), TH (C,I,O,U), EdU (D,J,P,V) and Ki67 (E,K,Q,W). Overlay is shown in F,L,R,X. Medial domains of $Shh^{Cre};Wnt1^{\Delta vMes/\Delta vMes};R26^{tdTomato}$ mutants had more cells in the active cell cycle at E11.5 ($Ki67^+$, white arrows) compared with controls. Fewer cells exited the cell cycle and differentiated into MbDA neurons ($EdU^+/TH^+/Ki67^-$, white arrowheads) in mutants versus controls. Yellow arrowheads indicate $Edu^+/TH^-/Ki67^-$ cells. Off-midline domains of $Shh^{Cre};Wnt1^{\Delta vMes/\Delta vMes};R26^{tdTomato}$ mutants showed increased MbDA neurons birthdated at E11.5 ($EdU^+/TH^+/Ki67^-$, white arrowheads). MbDA neurons born outside the range of EdU kinetics were $EdU^-/TH^+/Ki67^-$ (yellow arrows). Dashed line indicates boundary between ventricular zone (VZ) and differentiated zone (DZ). (**Y-Z'**) Quantitative assessment of $Shh^{Cre};Wnt1^{\Delta vMes/+};R26^{tdTomato}$ controls (dark gray bars) and $Shh^{Cre};Wnt1^{vMes/vMes};R26^{tdTomato}$ mutants (light gray bars) at E12.5. (Y,Y') Total, rostral, intermediate and caudal MbDA neurons birthdated at E11.5 (TH^+EdU^+) in medial and off-midline planes. (Z,Z') Ratio of MbDA neurons born at E11.5 ($TH^+EdU^+Ki67^-$) to the total number of cells born at E11.5 (EdU^+Ki67^-). $^*P<0.05$, $^{**}P<0.01$, $^{***}P<0.001$. Error bars represent s.d. (**AA**) Illustration of cell cycle exit data. At E11.5, $Ki67^+$ cells (green cells) proliferate in the VZ, subsequently migrate along radial glia (beige cells), and differentiate into TH^+ MbDA neurons (gold neurons); the early born MbDA neurons are located more lateral than the later born MbDA neurons. The addition of EdU at E11.5 tracks differentiating MbDA neurons (red shading, gold neurons). In $ShhCre;Wnt1^{\Delta vMes/+}$ embryos, $TH^+/Edu^+/Ki67^-$ MbDA neurons were primarily located in a medial location whereas TH+Edu-/Ki67- MbDA neurons were located laterally. The conditional deletion of *Wnt1* in $ShhCre;Wnt1^{\Delta vMes/\Delta vMes}$ embryos disrupted the timing of cell cycle exit, which caused the depletion of medial MbDA neurons and a concomitant increase of ectopic, laterally positioned $TH^+/Edu^+/Ki67^-$ MbDA neurons.

WNT signaling can antagonize *Shh* expression (Joksimovic et al., 2009). However, our early deletion of *Wnt1* shows that *Shh* expression is not increased and suggests that WNT1 does not drive canonical WNT-mediated antagonism of *Shh* in the v.Mes and that the phenotype we observe is not due to changes in *Shh*. It is possible that the early deletion of *Wnt1* and the near-complete loss of MbDA

neurons were secondary to the changes in *Fgf8*. However, we do not believe that this is the case because, unlike our $En1^{Cre};Wnt1^{fl/fl}$ conditional mutants, which have a near-complete depletion of MbDA neurons at E12.5, the deletion of *Fgf8* (at the same time and using the same *Cre* line) in $En1^{Cre};Fgf8^{fl/fl}$ embryos results in a normal complement of TH^+ neurons at E12.5 (Ellisor et al., 2012). Interestingly, ES cells treated with SHH and FGF8 express *Wnt1* prior to becoming MbDA-like neurons (Lee et al., 2000) (M.Z., unpublished results) and *Wnt1* is important for SHH- and FGF8-mediated ectopic induction of MbDA neurons (Prakash and Wurst, 2006). Therefore, the role of *Wnt1* in MbDA neuron development is independent of *Fgf8* and *Shh*, although future experiments are needed to address how the convergence of FGF8, SHH and WNT1 signaling shapes MbDA neuron progenitors.

Deletion of *Wnt1* in the *Shh* lineage ($Shh^{Cre};Wnt1^{fl/fl}$) reveals that OTX2, LMX1a and NURR1 are unaffected, which is similar to observations in Shh^{Cre};β-$catenin^{fl/fl}$ mice described by Tang et al. (Tang et al., 2009) using the same Shh^{Cre} line. We show that the cell cycle of only MbDA neurons are affected in our conditional *Wnt1* mutants as reflected in the decreased ratio of MbDA neurons/all cells born. By contrast, conditional β-catenin mutants have a decrease in the birthdating of all cells, including MbDA neurons. These findings suggest that disrupting β-catenin-dependent WNT signaling causes a more global disruption of cells going through S phase than does the deletion of WNT1 ligand alone. The reduction of MbDA neurons born at E11.5 is similar in conditional β-catenin and our conditional *Wnt1* mutants (~50% decrease in E11.5-born MbDA neurons in both mutants), suggesting that cell cycle progression and neurogenesis of MbDA neurons is largely mediated by WNT1 via canonical signaling. Interestingly, disruption of the cell cycle is linked to the depletion of differentiated MbDA neurons (as shown by decreased total numbers of TH^+ neurons), and *Wnt1* deletion in the v.Mes results in MbDA neurons that are displaced and improperly positioned, which may be due to changes in cell migration. Although this may shape MbDA neuron subtype identity, the early phenotype we observe does not directly address whether *Wnt1* and cell cycle alteration affects ventral tegmental area (VTA) or substantia nigra (SNc) identity in adults, which will be important to resolve in future studies. In summary, our analyses reveal that *Wnt1* is an important regulatory component that controls cell cycle exit and resolve the spatial and temporal roles for *Wnt1* in specific developmental processes and in MbDA neurons during embryogenesis.

Acknowledgements
We thank M. Furey for karyotyping of ES cells and ES cell culture; and Dr Ahn and Dr Wang for advice on EdU and Ki67 experiments.

Funding
This research and publication was funded by the National Institutes of Health National Institute of General Medical Sciences (NIH/NIGMS) [grant #8P20GM103468-04]. Deposited in PMC for release after 12 months.

Competing interests statement
The authors declare no competing financial interests.

Author contributions
$Wnt1^{fl}$ allele work was carried out by J.Y. and D.E.; ES cell work by E.P. and D.E.; $En1^{Cre}$-mediated deletion of $Wnt1^{fl}$ and qRT-PCR by D.E. and M.Z.; $Gbx2^{CreER\text{-}ires\text{-}eGFP}$ experiments by N.H.; and *Wnt1-CreER* and Shh^{Cre} experiments by A.B. The paper was written by M.Z., D.E. and A.B.

Supplementary material
Supplementary material available online at
http://dev.biologists.org/lookup/suppl/doi:10.1242/dev.080630/-/DC1

References

Andersson, E., Tryggvason, U., Deng, Q., Friling, S., Alekseenko, Z., Robert, B., Perlmann, T. and Ericson, J. (2006). Identification of intrinsic determinants of midbrain dopamine neurons. *Cell* **124**, 393-405.
Ang, S. L. (2006). Transcriptional control of midbrain dopaminergic neuron development. *Development* **133**, 3499-3506.
Bally-Cuif, L., Cholley, B. and Wassef, M. (1995). Involvement of Wnt-1 in the formation of the mes/metencephalic boundary. *Mech. Dev.* **53**, 23-34.
Bayer, S. A., Wills, K. V., Triarhou, L. C. and Ghetti, B. (1995). Time of neuron origin and gradients of neurogenesis in midbrain dopaminergic neurons in the mouse. *Exp. Brain Res.* **105**, 191-199.
Blaess, S., Bodea, G. O., Kabanova, A., Chanet, S., Mugniery, E., Derouiche, A., Stephen, D. and Joyner, A. L. (2011). Temporal-spatial changes in Sonic Hedgehog expression and signaling reveal different potentials of ventral mesencephalic progenitors to populate distinct ventral midbrain nuclei. *Neural Dev.* **6**, 29.
Brown, A., Brown, S., Ellisor, D., Hagan, N., Normand, E. and Zervas, M. (2009). A practical approach to genetic inducible fate mapping: a visual guide to mark and track cells in vivo. *J. Vis. Exp.* **2009**, 1687.
Brown, A., Machan, J. T., Hayes, L. and Zervas, M. (2011). Molecular organization and timing of Wnt1 expression define cohorts of midbrain dopamine neuron progenitors in vivo. *J. Comp. Neurol.* **519**, 2978-3000.
Bye, C. R., Thompson, L. H. and Parish, C. L. (2012). Birth dating of midbrain dopamine neurons identifies A9 enriched tissue for transplantation into parkinsonian mice. *Exp. Neurol.* **236**, 58-68.
Chen, L., Guo, Q. and Li, J. Y. H. (2009). Transcription factor Gbx2 acts cell-nonautonomously to regulate the formation of lineage-restriction boundaries of the thalamus. *Development* **136**, 1317-1326.
Chi, C. L., Martinez, S., Wurst, W. and Martin, G. R. (2003). The isthmic organizer signal FGF8 is required for cell survival in the prospective midbrain and cerebellum. *Development* **130**, 2633-2644.
Chung, S., Leung, A., Han, B. S., Chang, M. Y., Moon, J. I., Kim, C. H., Hong, S., Pruszak, J., Isacson, O. and Kim, K. S. (2009). Wnt1-lmx1a forms a novel autoregulatory loop and controls midbrain dopaminergic differentiation synergistically with the SHH-FoxA2 pathway. *Cell Stem Cell* **5**, 646-658.
Di Salvio, M., Di Giovannantonio, L. G., Acampora, D., Prosperi, R., Omodei, D., Prakash, N., Wurst, W. and Simeone, A. (2010). Otx2 controls neuron subtype identity in ventral tegmental area and antagonizes vulnerability to MPTP. *Nat. Neurosci.* **13**, 1481-1488.
Echelard, Y., Vassileva, G. and McMahon, A. P. (1994). Cis-acting regulatory sequences governing Wnt-1 expression in the developing mouse CNS. *Development* **120**, 2213-2224.
Ellisor, D., Koveal, D., Hagan, N., Brown, A. and Zervas, M. (2009). Comparative analysis of conditional reporter alleles in the developing embryo and embryonic nervous system. *Gene Expr. Patterns* **9**, 475-489.
Ellisor, D., Rieser, C., Voelcker, B., Machan, J. T. and Zervas, M. (2012). Genetic dissection of midbrain dopamine neuron development in vivo. *Dev. Biol.* **372**, 249-262.
Hagan, N. and Zervas, M. (2012). Wnt1 expression temporally allocates upper rhombic lip progenitors and defines their terminal cell fate in the cerebellum. *Mol. Cell. Neurosci.* **49**, 217-229.
Harfe, B. D., Scherz, P. J., Nissim, S., Tian, H., McMahon, A. P. and Tabin, C. J. (2004). Evidence for an expansion-based temporal Shh gradient in specifying vertebrate digit identities. *Cell* **118**, 517-528.
Hayes, L., Zhang, Z., Albert, P., Zervas, M. and Ahn, S. (2011). Timing of Sonic hedgehog and Gli1 expression segregates midbrain dopamine neurons. *J. Comp. Neurol.* **519**, 3001-3018.
Joksimovic, M., Anderegg, A., Roy, A., Campochiaro, L., Yun, B., Kittappa, R., McKay, R. and Awatramani, R. (2009). Spatiotemporally separable Shh domains in the midbrain define distinct dopaminergic progenitor pools. *Proc. Natl. Acad. Sci. USA* **106**, 19185-19190.
Kawano, H., Ohyama, K., Kawamura, K. and Nagatsu, I. (1995). Migration of dopaminergic neurons in the embryonic mesencephalon of mice. *Brain Res. Dev. Brain Res.* **86**, 101-113.
Kimmel, R. A., Turnbull, D. H., Blanquet, V., Wurst, W., Loomis, C. A. and Joyner, A. L. (2000). Two lineage boundaries coordinate vertebrate apical ectodermal ridge formation. *Genes Dev.* **14**, 1377-1389.
Lee, S. H., Lumelsky, N., Studer, L., Auerbach, J. M. and McKay, R. D. (2000). Efficient generation of midbrain and hindbrain neurons from mouse embryonic stem cells. *Nat. Biotechnol.* **18**, 675-679.
Li, J. Y., Lao, Z. and Joyner, A. L. (2002). Changing requirements for Gbx2 in development of the cerebellum and maintenance of the mid/hindbrain organizer. *Neuron* **36**, 31-43.
Liu, P., Jenkins, N. A. and Copeland, N. G. (2003). A highly efficient recombineering-based method for generating conditional knockout mutations. *Genome Res.* **13**, 476-484.
Luu, B., Ellisor, D. and Zervas, M. (2011). The lineage contribution and role of Gbx2 in spinal cord development. *PLoS ONE* **6**, e20940.
Madisen, L., Zwingman, T. A., Sunkin, S. M., Oh, S. W., Zariwala, H. A., Gu, H., Ng, L. L., Palmiter, R. D., Hawrylycz, M. J., Jones, A. R. et al. (2010). A robust

and high-throughput Cre reporting and characterization system for the whole mouse brain. *Nat. Neurosci.* **13**, 133-140.
McMahon, A. P. and Bradley, A. (1990). The Wnt-1 (int-1) proto-oncogene is required for development of a large region of the mouse brain. *Cell* **62**, 1073-1085.
McMahon, A. P., Joyner, A. L., Bradley, A. and McMahon, J. A. (1992). The midbrain-hindbrain phenotype of Wnt-1-/Wnt-1- mice results from stepwise deletion of engrailed-expressing cells by 9.5 days postcoitum. *Cell* **69**, 581-595.
Omodei, D., Acampora, D., Mancuso, P., Prakash, N., Di Giovannantonio, L. G., Wurst, W. and Simeone, A. (2008). Anterior-posterior graded response to Otx2 controls proliferation and differentiation of dopaminergic progenitors in the ventral mesencephalon. *Development* **135**, 3459-3470.
Ono, Y., Nakatani, T., Sakamoto, Y., Mizuhara, E., Minaki, Y., Kumai, M., Hamaguchi, A., Nishimura, M., Inoue, Y., Hayashi, H. et al. (2007). Differences in neurogenic potential in floor plate cells along an anteroposterior location: midbrain dopaminergic neurons originate from mesencephalic floor plate cells. *Development* **134**, 3213-3225.
Pettitt, S. J., Liang, Q., Rairdan, X. Y., Moran, J. L., Prosser, H. M., Beier, D. R., Lloyd, K. C., Bradley, A. and Skarnes, W. C. (2009). Agouti C57BL/6N embryonic stem cells for mouse genetic resources. *Nat. Methods* **6**, 493-495.
Prakash, N. and Wurst, W. (2006). Genetic networks controlling the development of midbrain dopaminergic neurons. *J. Physiol.* **575**, 403-410.
Soldner, F., Hockemeyer, D., Beard, C., Gao, Q., Bell, G. W., Cook, E. G., Hargus, G., Blak, A., Cooper, O., Mitalipova, M. et al. (2009). Parkinson's disease patient-derived induced pluripotent stem cells free of viral reprogramming factors. *Cell* **136**, 964-977.
Tang, M., Miyamoto, Y. and Huang, E. J. (2009). Multiple roles of beta-catenin in controlling the neurogenic niche for midbrain dopamine neurons. *Development* **136**, 2027-2038.
Tang, M., Villaescusa, J. C., Luo, S. X., Guitarte, C., Lei, S., Miyamoto, Y., Taketo, M. M., Arenas, E. and Huang, E. J. (2010). Interactions of Wnt/beta-catenin signaling and sonic hedgehog regulate the neurogenesis of ventral midbrain dopamine neurons. *J. Neurosci.* **30**, 9280-9291.
Thomas, K. R. and Capecchi, M. R. (1990). Targeted disruption of the murine int-1 proto-oncogene resulting in severe abnormalities in midbrain and cerebellar development. *Nature* **346**, 847-850.
Thomas, K. R., Musci, T. S., Neumann, P. E. and Capecchi, M. R. (1991). Swaying is a mutant allele of the proto-oncogene Wnt-1. *Cell* **67**, 969-976.
Vernay, B., Koch, M., Vaccarino, F., Briscoe, J., Simeone, A., Kageyama, R. and Ang, S. L. (2005). Otx2 regulates subtype specification and neurogenesis in the midbrain. *J. Neurosci.* **25**, 4856-4867.
Wang, H., Ge, G., Uchida, Y., Luu, B. and Ahn, S. (2011). Gli3 is required for maintenance and fate specification of cortical progenitors. *J. Neurosci.* **31**, 6440-6448.
Wexler, E. M., Rosen, E., Lu, D., Osborn, G. E., Martin, E., Raybould, H. and Geschwind, D. H. (2011). Genome-wide analysis of a Wnt1-regulated transcriptional network implicates neurodegenerative pathways. *Sci. Signal.* **4**, ra65.
Wilkinson, D. G., Bailes, J. A. and McMahon, A. P. (1987). Expression of the proto-oncogene int-1 is restricted to specific neural cells in the developing mouse embryo. *Cell* **50**, 79-88.
Ye, W., Shimamura, K., Rubenstein, J. L., Hynes, M. A. and Rosenthal, A. (1998). FGF and Shh signals control dopaminergic and serotonergic cell fate in the anterior neural plate. *Cell* **93**, 755-766.
Zervas, M., Millet, S., Ahn, S. and Joyner, A. L. (2004). Cell behaviors and genetic lineages of the mesencephalon and rhombomere 1. *Neuron* **43**, 345-357.
Zervas, M., Blaess, S. and Joyner, A. L. (2005). Classical embryological studies and modern genetic analysis of midbrain and cerebellum development. *Curr. Top. Dev. Biol.* **69**, 101-138.